

How to Make Dull Cellular Automata Complex by Adding Memory: Rule 126 Case Study

GENARO J. MARTÍNEZ,^{1,2} ANDREW ADAMATZKY,² JUAN C. SECK-TUOH-MORA,³ AND RAMON ALONSO-SANZ^{2,4}

¹Departamento de Gravitación, Instituto de Ciencias Nucleares, Universidad Nacional Autónoma de México, México; ²Department of Computer Science, Bristol Institute of Technology, University of the West of England, Bristol, United Kingdom; ³Tecnologías Avanzadas en Ingeniería, Centro de Investigación Avanzada en Ingeniería Industrial, Universidad Autónoma del Estado de Hidalgo, México; and ⁴Departamento de Estadística y Métodos de Gestión en Agricultura, ETSI Agrónomos, Polytechnic University of Madrid, Madrid, Spain

Received July 14, 2009; revised December 2, 2009; accepted December 16, 2009

Using Rule 126 elementary cellular automaton (ECA), we demonstrate that a chaotic discrete system — when enriched with memory — hence exhibits complex dynamics where such space exploits on an ample universe of periodic patterns induced from original information of the ahistorical system. First, we analyze classic ECA Rule 126 to identify basic characteristics with mean field theory, basins, and de Bruijn diagrams. To derive this complex dynamics, we use a kind of memory on Rule 126; from here interactions between gliders are studied for detecting stationary patterns, glider guns, and simulating specific simple computable functions produced by glider collisions. © 2010 Wiley Periodicals, Inc. *Complexity* 15: 34–49, 2010

Key Words: elementary cellular automata; memory; Rule 126; gliders; glider guns; filters; chaos; complex dynamics

1. INTRODUCTION

In this article, we are making use of the memory tool to get a complex system from a chaotic function in discrete dynamical environments. Such technique takes the past history of the system for constructing its present and future: the memory [1–6]. It was previously reported in [7] how the chaotic elementary cellular automaton (ECA) Rule

30 is decomposed into a complex system applying memory on this function. Recent results show that other chaotic functions (Rule 86 and Rule 101) yield complex dynamics selecting a kind of memory, including a controller to obtain self-organization by structure reactions and simple computations implemented by soliton reactions [8].

We focus this work on cellular automata (CA) evolving in one dimension, in particular taking the well-known ECA where each function evaluates a central cell and its two nearest neighbors (from left and right), and every cell takes a value from a binary alphabet. Such ECA were introduced by Wolfram and have been widely studied in several directions [9].

Correspondence to: Genaro J. Martínez, Instituto de Ciencias Nucleares, Universidad Nacional Autónoma de México, México. (e-mail: genaro.martinez@uwe.ac.uk)

Among such ECA, there is a set of functions evolving in chaotic global behavior where a number of cells remain unordered and their transitions have a large number of ancestors [10]. In this sense, special attention is given on a chaotic one: the ECA Rule 126 introduced by Wolfram in [11]. Particularly in [12],¹ it is commented that Rule 126 generates a regular language with average growing faster than any polynomial time. This property can be analyzed as well by de Bruijn diagrams with additional features; in particular, another partial analysis with de Bruijn and subset diagrams was done by McIntosh [13] showing that string 010 in Rule 126 is the minimal Garden of Eden configuration (having no ancestors).

Based on the idea developed in previous results for obtaining complex dynamics from chaotic functions selecting memory and working systematically, it was suspected that a complex dynamics may emerge in Rule 126 given its relation to regular languages; making use of gliders coded by regular expressions, as it was studied in Rule 110 [14] and Rule 54 [15].

In this way, Rule 126 provides a special case of how a chaotic behavior can be decomposed selecting a kind of memory into an extraordinary activity of gliders, glider guns, still-life structures, and a huge number of reactions. Such features can be compared to Brain Brian's rule behavior or Conway's Life but in one dimension; actually none traditional ECA could have a glider dynamics comparable to the one revealed in this ECA with memory denoted as $\phi_{R126maj}$ (following notation described in [7, 8]).

1.1. One-Dimensional Cellular Automata

One-dimensional CA is represented by an array of *cells* x_i where $i \in \mathbb{Z}$ (integer set) and each x takes a value from a finite alphabet Σ . Thus, a sequence of cells $\{x_i\}$ of finite length n describes a string or global configuration c on Σ . This way, the set of finite configurations will be expressed as Σ^n . An evolution is comprised by a sequence of configurations $\{c_i\}$ produced by the mapping $\Phi : \Sigma^n \rightarrow \Sigma^n$; thus, the global relation is symbolized as:

$$\Phi(c^t) \rightarrow c^{t+1}, \quad (1)$$

where t represents time and every global state of c is defined by a sequence of cell states. The global relation is determined over the cell states in configuration c^t updated at the next configuration c^{t+1} simultaneously by a local function φ as follows:

$$\varphi(x_{i-r}^t, \dots, x_i^t, \dots, x_{i+r}^t) \rightarrow x_i^{t+1}. \quad (2)$$

Wolfram represents one-dimensional CA with two parameters (k, r) , where $k = |\Sigma|$ is the number of states, and r

¹<http://mathworld.wolfram.com/Rule126.html>

is the neighborhood radius, hence ECA domain is defined by parameters $(2, 1)$. There are Σ^n different neighborhoods (where $n = 2r + 1$) and k^{k^n} distinct evolution rules. The evolutions in this article have periodic boundary conditions.

1.2. Cellular Automata with Memory

Conventional CA are ahistoric (memoryless): i.e., the new state of a cell depends on the neighborhood configuration solely at the preceding time step of φ . CA with memory can be considered as an extension of the standard framework of CA where every cell x_i is allowed to remember some period of its previous evolution. Basically, memory is based on the state and history of the system, thus we design a memory function ϕ , as follows:

$$\phi(x_i^{t-\tau}, \dots, x_i^{t-1}, x_i^t) \rightarrow s_i \quad (3)$$

such that $\tau < t$ determines the backward degree of memory and each cell $s_i \in \Sigma$ is a function of the series of states in cell x_i up to time-step $t - \tau$. Finally, to execute the evolution we apply the original rule again as follows:

$$\varphi(\dots, s_{i-1}^t, s_i^t, s_{i+1}^t, \dots) \rightarrow x_i^{t+1}.$$

In CA with memory, while the mapping φ remains unaltered, a historic memory of past iterations is retained by featuring each cell as a summary of its previous states; therefore, cells canalize memory to the map φ . As an example, we can take the memory function ϕ as a majority memory:

$$\phi_{maj} \rightarrow s_i \quad (4)$$

So, ϕ_{maj} represents the classic majority function for three variables [16], as follows:

$$\phi_{maj} : (x_1 \wedge x_2) \vee (x_2 \wedge x_3) \vee (x_3 \wedge x_1) \rightarrow x$$

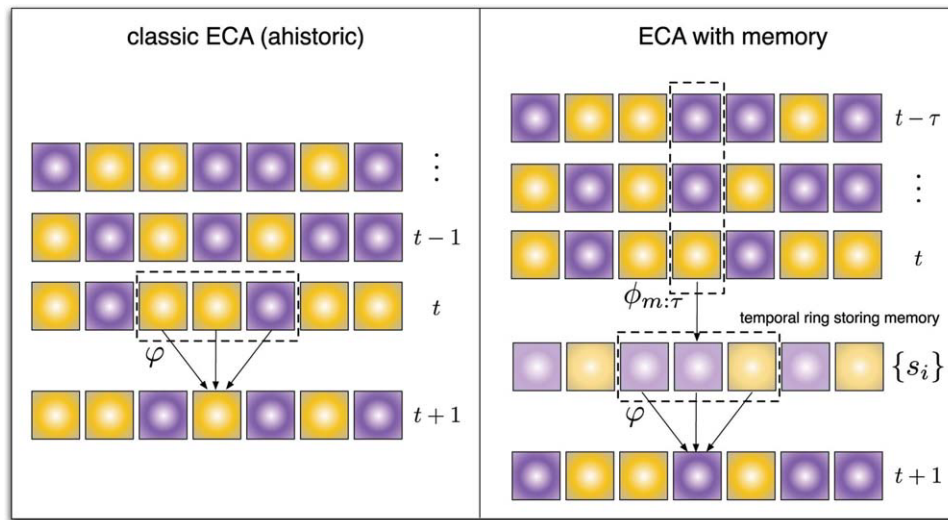
on cells $(x_i^{t-\tau}, \dots, x_i^{t-1}, x_i^t)$ and defines a temporal ring before calculating the next global configuration c . In case of a tie, it allows to break it in favor of zero if $x_{\tau-1} = 0$, or to one whether $x_{\tau-1} = 1$. The representation of a ECA with memory (given previously in [7, 8]) is given as follows:

$$\phi_{CARm:\tau} \quad (5)$$

where CAR represents the decimal notation of a particular ECA and m the kind of memory given with a specific value of τ . Thus, the majority memory (maj) working in ECA Rule 126 checking tree cells ($\tau = 3$) of history is simply denoted as $\phi_{R126maj:3}$. Figure 1 depicts in detail the memory working on ECA.

Note that memory is as simple as any CA local function but sometimes the global behavior produced by the local rule is totally unpredictable.

FIGURE 1



Cellular automata with memory in cells.

1.2.1. Disclaimer

The memory mechanism considered here differs from other CA with memory previously reported, often referred as higher order (in-time) CA.² These ones, in most cases, explicitly alter the function ϕ and incorporate memory by directly determining the new configuration in terms of the configurations at previous time-steps. Thus, in second order in time (memory of capacity two) rules, the transition rule operates as: $x^{t+1} = \Phi(c^t, c^{t-1})$. Double memory (in transition rule and in cells) can be implemented as: $x^{t+1} = \Phi(\{s^t\}, \{s^{t-1}\})$. Particularly interesting is the reversible formulation: $x^{t+1} = \phi \ominus x^{t-1}$; reversible CA with memory are studied in [6].

Some authors define rules with memory as those with dependence in ϕ on the state of the cell to be updated [20,21]. So, one-dimensional rules with no memory adopt the form: $x^{t+1} = \phi(x_{i-1}^t, x_{i+1}^t)$. Memory is not here identified with delay, i.e., referring cells exclusively to their state values a number of time-steps in the past, [22]. So, for example, the cell to be updated may be referenced not at t but at $t - 1$: $x^{t+1} = \phi(x_{i-1}^t, x_i^t, x_{i+1}^t)$ [23]. Again, the mapping function is not extended, for example, to consider the influence of cell i at time $t - 1$: $x^{t+1} = \psi(x_{i-1}^{t-1}, x_{i-1}^t, x_i^t, x_{i+1}^t)$ as done in [24].

The use of the locution associative memory usually refers, when used in the CA context, to the study of configuration attractors [25, 26], which are argued by Wuensche [27] to constitute the network's global states contents addressable memory in the sense of Hopfield [28].

²See, for example, [17] p. 118; [18] p. 43; or class MEMO in [19] p. 7.

Finally, it is not intended here to emulate human memory, i.e., the associative, pattern matching, highly parallel function of human memory. The aim is just to store the past, or just a part of it, to make it work in dynamics. Thus, working storage might replace here the use of the term memory, avoiding the anthropomorphic, and rather unavoidable, connotations of the word memory [6].

2. THE BASIC FUNCTION: ECA RULE 126

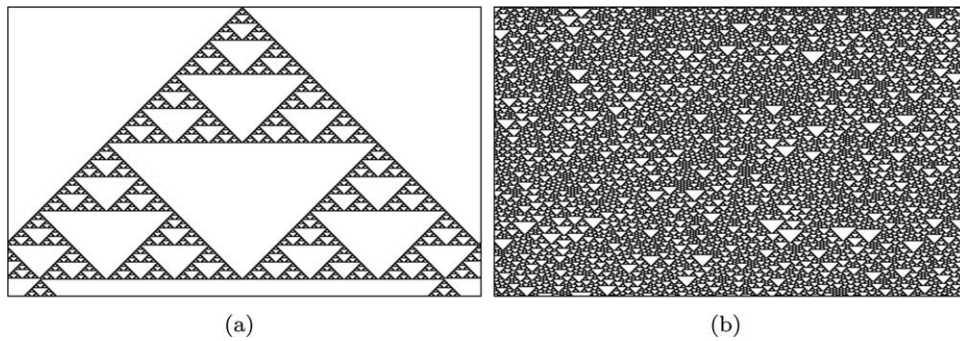
The local-state transition function ϕ corresponding to Rule 126 is represented as follows:

$$\phi_{R126} = \begin{cases} 1 & \text{if } 110, 101, 100, 011, 010, 001 \\ 0 & \text{if } 111, 000 \end{cases}$$

Rule 126 has a chaotic global behavior typical from Class III in Wolfram's classification [9]. In ϕ_{R126} we can easily recognize an initial high probability of alive cells, i.e., cells in state "1"; with a 75% to appear in the next time and complement of only 25% to get state 0. It will be always a new alive cell iff ϕ_{R126} has one or two alive cells such that the equilibrium comes when there is an overpopulation condition. Figure 2 shows these cases in typical evolutions of Rule 126, both evolving from a single cell in state "1" [Figure 2(a)] and from a random initial configuration [Figure 2(b)] where a high density of 1's is evidently in the evolution.

While looking on chaotic space-time configuration in Figure 2, we understand the difficulty for analyzing the rule's behavior and selecting any coherent activity among periodic structures without special tools.

FIGURE 2



Typical fractal (a) and chaotic (b) global evolution of ECA Rule 126. (a) Initially all cells in “0” but one in state “1,” (b) evolution from random initial configuration with 50% of “0” and “1” states.

2.1. Mean Field Approximation in ECA Rule 126

This section presents a probabilistic analysis with mean field theory to search basic properties about φ_{R126} evolution space and its related chaotic behavior. Such analysis will offer a better spectrum where we can start to explore the evolution space from more useful and specific initial conditions where some interesting behaviors may emerge.

Mean field theory is a well-known technique for discovering statistical properties of CA without analyzing evolution spaces of individual rules [13]. The method assumes that states in Σ are independent and do not correlate each other in the local function φ_{R126} . Thus, we can study probabilities of states in a neighborhood in terms of the probability of a single state (the state in which the neighborhood evolves), and probability of the neighborhood is product of the probabilities of each cell in it.

In this way, [29] presents an explanation of Wolfram’s classes by a mixture of probability theory and de Bruijn diagrams, resulting a classification based on mean field theory curve:

- class I: monotonic, entirely on one side of diagonal;
- class II: horizontal tangency, never reaches diagonal;
- class IV: horizontal plus diagonal tangency, no crossing;
- class III: no tangencies, curve crosses diagonal.

For the one-dimensional case, all neighborhoods are considered as follows:

$$p_{t+1} = \sum_{j=0}^{k^{2r+1}-1} \varphi_j(X) p_t^v (1 - p_t)^{n-v} \quad (6)$$

such that j is an index number relating each neighborhood and X are cells $x_{i-r}, \dots, x_i, \dots, x_{i+r}$. Thus, n is the number of cells into every neighborhood, v indicates how often state “1” occurs in X , $n - v$ shows how often state “0” occurs in the

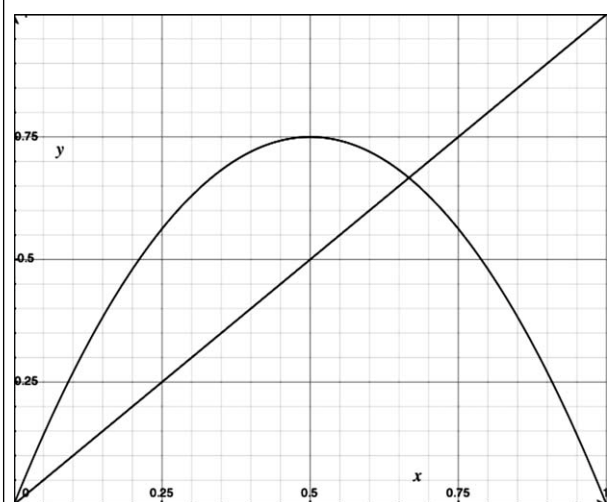
neighborhood X , p_t is the probability of cell being in state “1,” while q_t is the probability of cell being in state “0,” i.e., $q = 1 - p$. The polynomial for Rule 126 is defined as follows:

$$p_{t+1} = 3p_t q_t. \quad (7)$$

Because φ_{R126} is classified as a chaotic rule, we expect no tangencies and its curve must cross the identity; remembering that φ_{R126} has a 75% of probability to produce a state one.

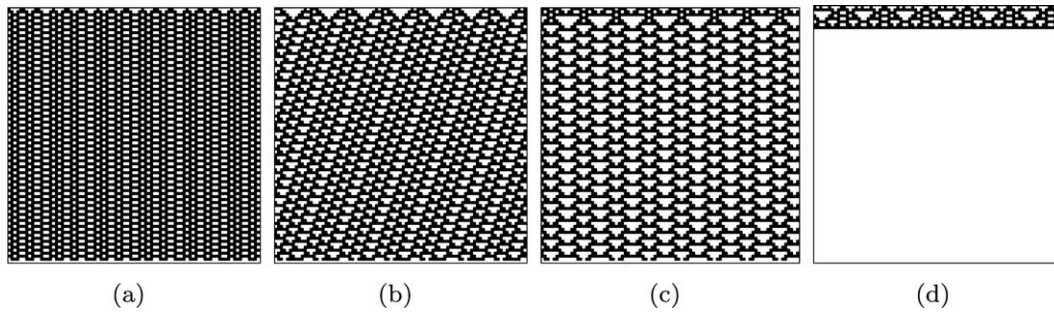
Mean field curve (Figure 3) confirms that probability of state “1” in space-time configurations of φ_{R126} is 0.75 for high densities related to big populations of 1’s. The curve also

FIGURE 3



Mean field curve for ECA Rule 126.

FIGURE 4



Periodic patterns from some basin attractors.

demonstrates that φ_{R126} is chaotic because the curve crosses the identity with a first fixed point at the origin $f = 0$ and the nonexistence of any unstable fixed point inducing non-stable regions in the evolution. Nevertheless, the stable fixed point is $f = 0.6683$, which represents a “concentration” of 1s diminishing during the automaton evolution.

Therefore, the initial inspection indicates no evidence of complex behavior emerging in φ_{R126} . Of course, a deeper analysis is necessary for obtaining more features from a chaotic rule, so the next sections explain other techniques to study in particular periodic structures.

2.2. Basins of Attraction

A basin (of attraction) field of a finite CA is the set of basins of attraction into which all possible states and trajectories will be organized by the local function φ . The topology of a single basin of attraction may be represented by a diagram, the state transition graph. Thus, the set of graphs composing the field specifies the global behavior of the system [30].

Generally, a basin can also recognize CA with chaotic or complex behavior following previous results on attractors [30]. Thus, we have that Wolfram’s classes can be represented as a basin classification:

- class I: very short transients, mainly point attractors (but possibly very periodic attractors) very high in-degree, and very high leaf density (very ordered dynamics);
- class II: very short transients, mainly short periodic attractors (but also point attractors), high in-degree, and very high leaf density;
- class IV: moderate transients, moderate-length periodic attractors, moderate in-degree, and very moderate leaf density (possibly complex dynamics);
- class III: very long transients, very long periodic attractors, low in-degree, and low leaf density (chaotic dynamics).

The basins depicted in Figure 5 show the whole set of non-equivalent basins in Rule 126 from $l = 2$ to $l = 18$ (l means

length of array) attractors, all they display not high densities from an attractor of mass one and attractors of mass 14.³ This way Rule 126 displays some nonsymmetric basins and some of them have long transients that induce a relation with chaotic rules.

Particularly we can see specific cycles in Figure 4 where it is possible to find:

- a. static configurations as still life patterns ($l = 8$);
- b. traveling configurations as gliders ($l = 15$);
- c. meshes ($l = 12$);
- d. or empty universes ($l = 14$).

The cycle diagrams expose only displacements to the left, and this empty universe evolving to the stable state 0 is constructed all times on the first basin for each cycle, see Figure 5.

This way some cycles could induce some nontrivial activity in Rule 126, but the associated initial conditions are not generally predominant. However, some information is useful indeed looking periodic patterns that have a high frequency inside this evolution space and hence for recognizing a kind of filter useful to get a better view of a possible complex activity in Rule 126.

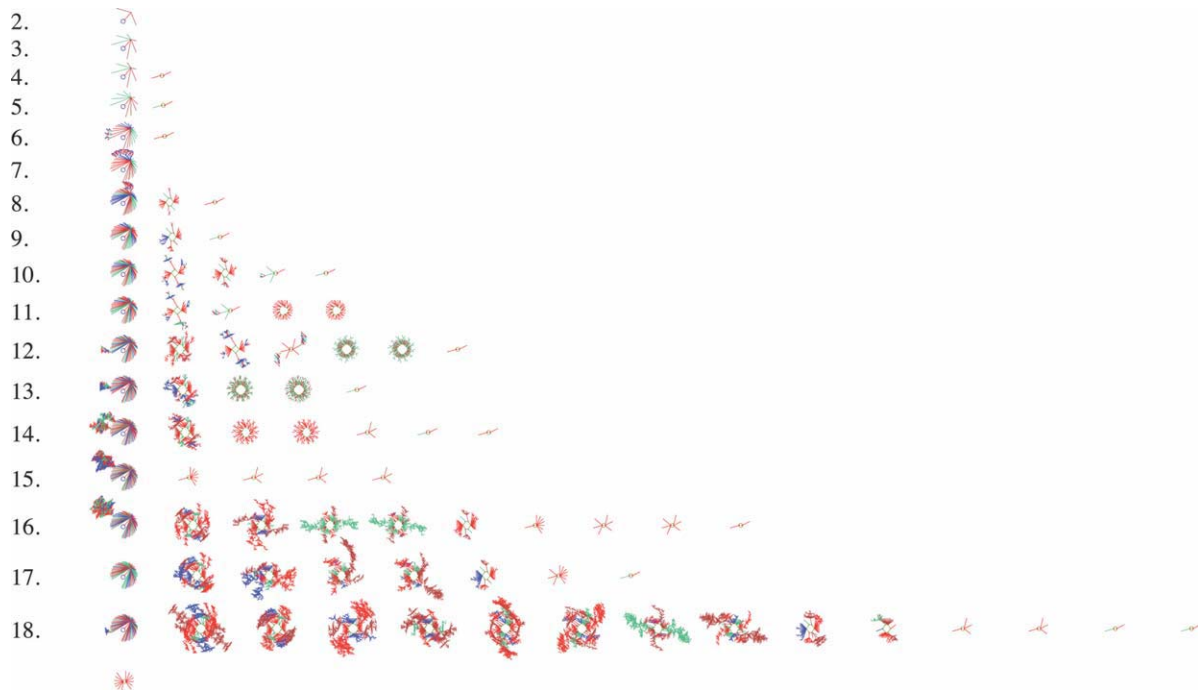
2.3. De Bruijn Diagrams

De Bruijn diagrams [13, 31] are very adequate for describing evolution rules in one-dimensional CA, although originally they were used in shift-register theory (the treatment of sequences where their elements overlap each other). Paths in a de Bruijn diagram may represent chains, configurations, or classes of configurations in the evolution space.

For a one-dimensional CA of order (k, r) , the de Bruijn diagram is defined as a directed graph with k^{2r} vertices and

³Basins and attractors were calculated with Discrete Dynamical System DDLab available from <http://www.ddlab.org/>.

FIGURE 5



The whole set of nonequivalent basins in ECA Rule 126 from $l = 2$ to $l = 18$.

k^{2r+1} edges. The vertices are labeled with the elements of the alphabet of length $2r$. An edge is directed from vertex i to vertex j , if and only if, the $2r - 1$ final symbols of i are the same that the $2r - 1$ initial ones in j forming a neighborhood of $2r + 1$ states represented by $i \diamond j$. In this case, the edge connecting i to j is labeled with $\varphi(i \diamond j)$ (the value of the neighborhood defined by the local function) [32].

The de Bruijn diagram associated to Rule 126 is depicted in Figure 6.⁴

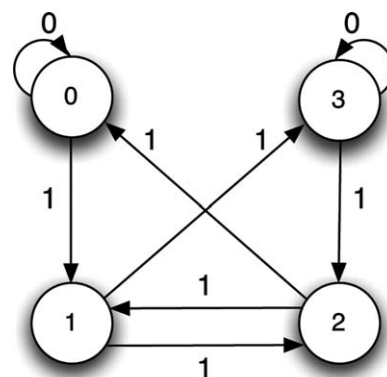
Figure 6 exposes that there are two neighborhoods evolving into 0 and six neighborhoods into 1, so the higher frequency is for state 1, indicating the possibility of having an injective automaton, that is, the existence of Garden of Eden configurations [13, 31]. Classical analysis in graph theory has been applied over de Bruijn diagrams for studying topics such as reversibility [33]; in other sense, cycles in the diagram indicate periodic constructions in the evolution of the automaton if the label of the cycle agrees with the sequence defined by its nodes, taking periodic boundary conditions. Let us take the equivalent construction of a de Bruijn diagram to describe

⁴De Bruijn diagrams were calculated using NXLCAU21 designed by Harold V. McIntosh; available from <http://delta.cs.cinvestav.mx/~mcintosh>.

the evolution in two steps of Rule 126 (having now nodes composed by sequences of four symbols); the cycles of this new diagram are presented in Figure 7.

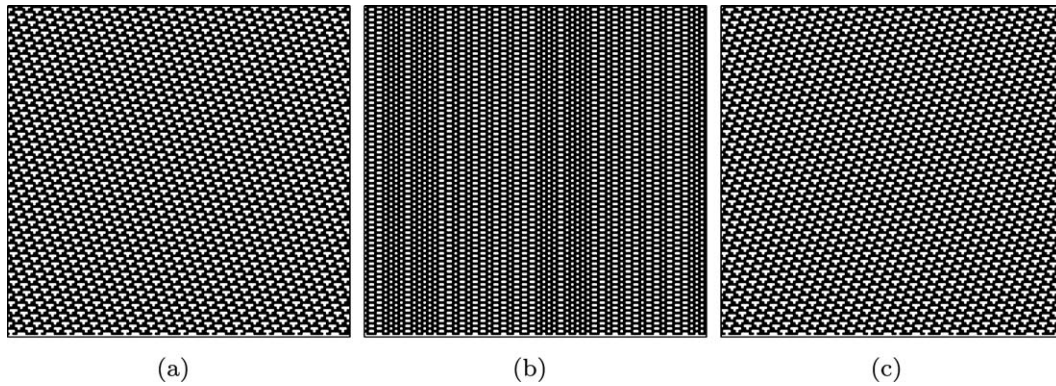
The extended de Bruijn diagrams [13] are useful for calculating all periodic sequences by the cycles defined in the diagram. These ones also show the shift of a sequence for a

FIGURE 6



De Bruijn diagram for the ECA Rule 126.

FIGURE 7



Patterns calculated from extended de Bruijn diagrams, in particular from cycles of order $(x, 2)$ (that means a x -shift in y -generations).

certain number of generations. Thus, we can get de Bruijn diagrams describing periodic sequences for Rule 126.

Cycles inside de Bruijn diagrams can be used for obtaining regular expressions representing a periodic pattern. Figure 7 displays three patterns calculated as: (a) shift -3 in 2 generations representing a pattern with displacement to the left, (b) shift 0 in 2 generations describing a static pattern traveling without displacement, and (c) shift $+3$ in 2 generations is exactly the symmetric pattern given in the first evolution.

So, we can also see in Figure 7 that it is possible to find patterns traveling in both directions, as gliders or mobile structures. However, generally, these constructions (strings) cannot live in combination with others structures, and therefore it is really hard to have this kind of objects with such characteristics. Although moreover Rule 126 has at least one glider! This will be explained in the next sections.

2.4. Filters for Recognizing Dynamics in Rule 126

Filters are a useful tool for discovering hidden order in chaotic or complex rules. Filters were introduced in CA studies by Wuensche who employed them to automatically classify cell-state transition functions, see [34]. Also filters related to tiles were successfully applied and deduced in analyzing space-time behavior of ECA governed by Rules 110 and 54 [15, 35, 36].

This way, we have found that Rule 126 has two types of two-dimensional tiles (which together work as filters over φ_{R126}):

- the tile $t_1 = \begin{bmatrix} 1111 \\ 1001 \end{bmatrix}$, and
- the tile $t_2 = \begin{bmatrix} 0000000 \\ 0111110 \\ 1100011 \\ 0110110 \\ 1111111 \end{bmatrix}$.

Filter t_1 works more significantly on configurations generated by φ_{R126} , the second one is not frequently found although it is exploited when Rule 126 is altered with memory (as we can see in following sections).

The application of the first filter is effective to discover gaps with little patterns traveling on triangles of '1' states in the evolution space. Although even in this case it may be unclear how a dynamics would be interpreted, a careful inspection on the evolution brings to light very small gliders (as still life), as shown in Figure 8.

This glider emerging in Rule 126 and localized by a filter is precisely the periodic pattern calculated with the basin [Figure 4(a)] and the de Bruijn diagram [Figure 7(b)]; in particular, the last one offers more information because such cycles allow to classify the whole phases when this glider is coded in the initial condition. The next sections demonstrate the effect of filters for recognizing an amazing universe evolving in this CA with memory.

3. CA $\phi_{R126maj:4}$ AND COMPLEX DYNAMICS

This section discusses both relevant aspects of classic Rule 126 (φ_{R126}) and Rule 126 with memory ($\phi_{R126m:\tau}$).

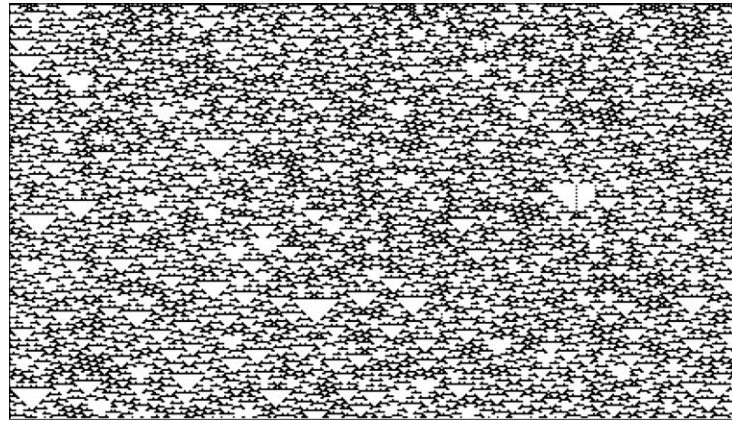
3.1. Dynamics Emerging with Majority Memory

As it was explained in [7, 37] a new family of evolution rules derived from classic ECA can be found selecting a kind of memory.

Figure 9 illustrates dynamics for some values of τ in $\phi_{R126maj:\tau}$.⁵ The space-time configurations are also filtered to show a raw dynamics. We found that large odd values of τ tend

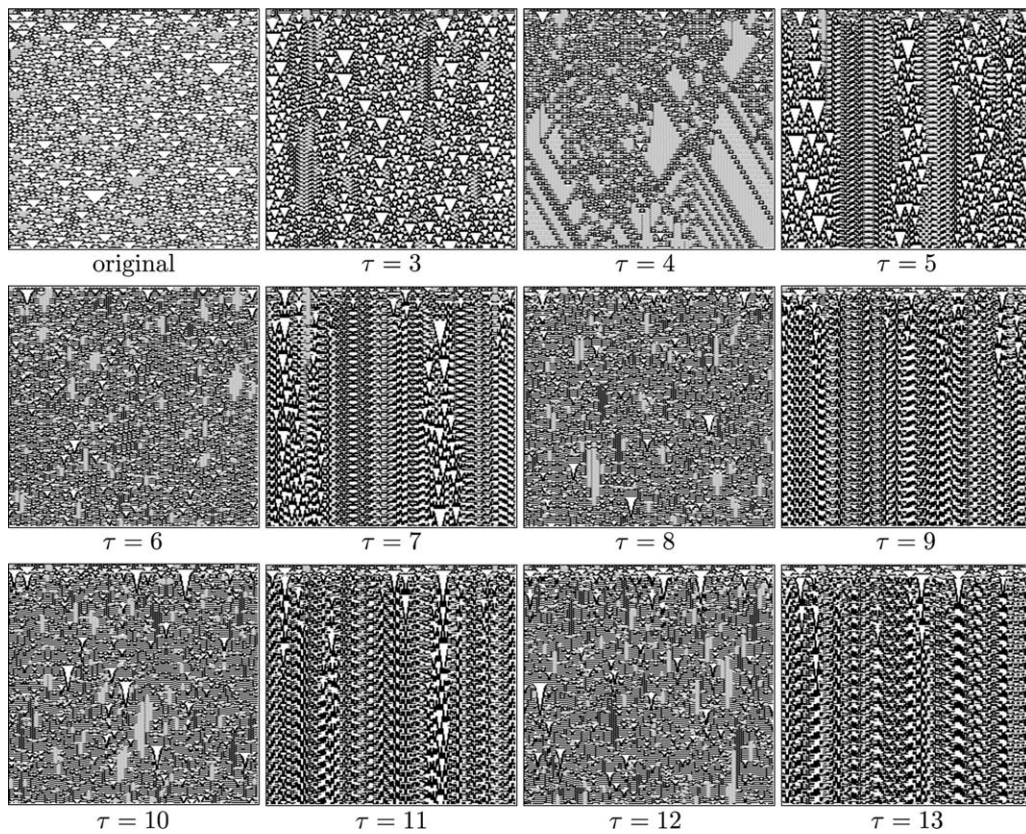
⁵*Evolutions of $\phi_{R126maj:\tau}$ were calculated with OSXL-CAU21 system available in <http://uncomp.uwe.ac.uk/genaro/OSXCASystems.html>.*

FIGURE 8



Filtered space-time configuration in ϕ_{R126} .

FIGURE 9



CA with majority memory $\phi_{R126\text{maj};\tau}$, where 13 values of τ are evolved and filtered over a ring of 246 cells for 236 generations.

to define macrocells-like patterns [9, 13]. Even values of τ are responsible of a mixture of periodic and chaotic dynamics.

On exploring systematically distinct values of τ , we found that $\phi_{R126maj:4}$ produces an impressive and nontrivial emergence of patterns traveling and colliding; so yet when the memory is working as a new function, it is possible to recognize some fragments inherited of the original rule ϕ_{R126} .

We start our simulations with a single nonquiescent cell, an example of this space-time configuration is provided in Figure 10 showing the first 1156 steps, where in this case the automaton needed other 12,000 steps to reach a stationary configuration. Filter is convenient to eliminate the nonrelevant information about gliders. In Figure 10 we can see a number of gliders, glider guns, still-life configurations, and a wide number of combinations of such patterns colliding and traveling with different velocities and densities. Consequently, we can classify a number of periodic structures, objects, and interesting reactions.

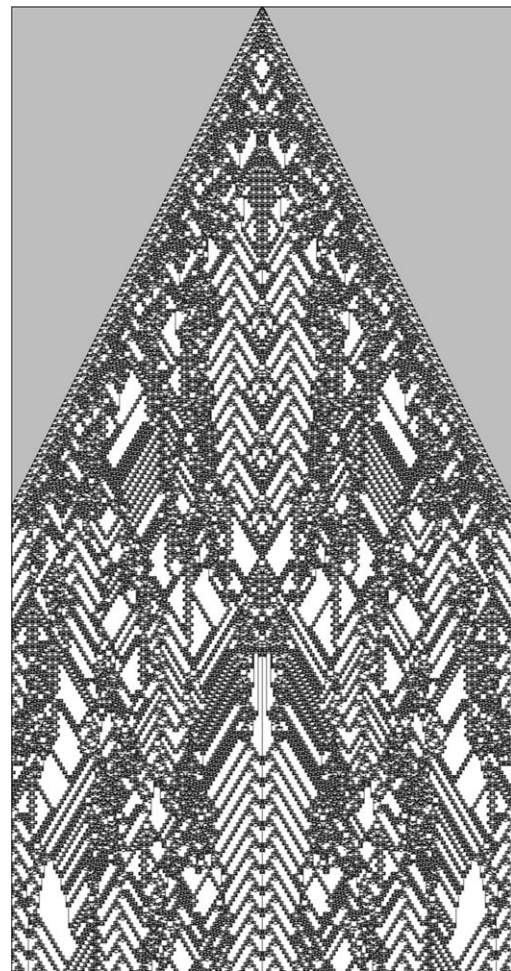
Basic primitive gliders are displayed in Figure 11, there are still-life patterns s_1 and s_2 , and gliders g_1 and g_2 , respectively. These structures can be ordered in a set $\mathcal{G}_{\phi_{R126maj:4}} = \{s_1, s_2, g_1, g_2\}$.

Figure 12 shows the three more frequent glider guns (gun_1 , gun_2 , and gun_3) emerging in $\phi_{R126maj:4}$. The next three guns [Figure 12(a-c)] are combined in basic guns synchronized by multiple reactions, which preserve emission of gliders although some of them can get other frequencies. We can include them increasing the set of periodic structures $\mathcal{G}_{\phi_{R126maj:4}} = \{s_1, s_2, g_1, g_2, gun_1, gun_2, gun_3, \text{ and } gun_4\}$. The last gun is presented in Figure 14 as a collision of gliders.

Basic properties of $\mathcal{G}_{\phi_{R126maj:4}}$ are given in Table 1, where also glider guns can be classified by frequencies of glider emission as follows:

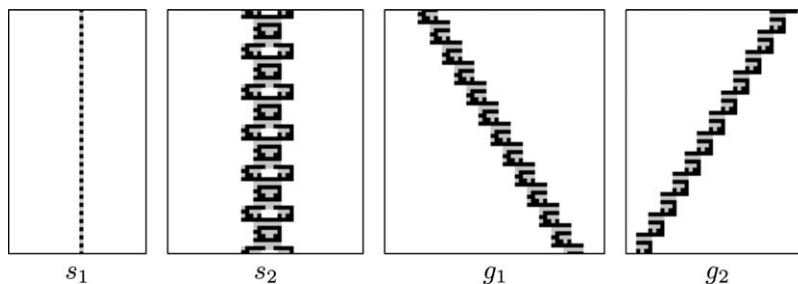
- small gun_1 fires a gliders g_1 and g_2 (in turn) every five steps;
- medium gun_2 fires g_1 and g_2 (in turn) every 26 steps;
- large gun_3 fires five g_1 and g_2 gliders every 100 steps.

FIGURE 10



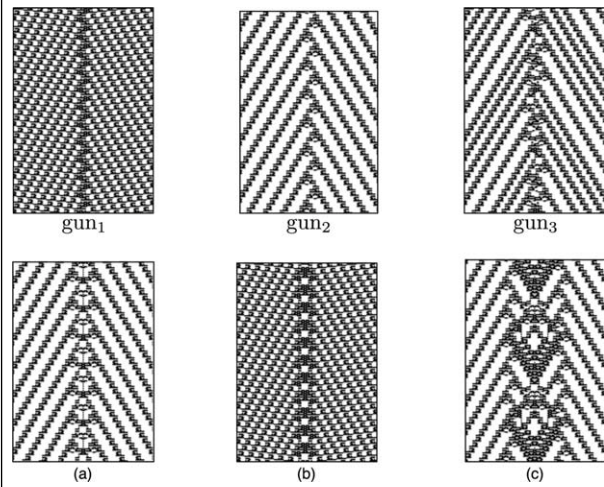
Filtered space-time configuration of $\phi_{R126maj:4}$ with 602 cells, periodic boundaries, starting from one nonquiescent cell and running for 1156 steps.

FIGURE 11



Basic gliders in $\phi_{R126maj:4}$. Two stationary configurations (as still life patterns) s_1 and s_2 , respectively, and two gliders g_1 and g_2 .

FIGURE 12



Samples of glider guns and their compositions in $\phi_{R126maj:4}$.

Frequencies are related to the number of emitted gliders (in intervals) by a glider gun. Hence, the gun_2 generates one g_1 and another g_2 glider eight steps before to produce the next ones, and a gun_3 yields five g_1 and five g_2 gliders 100 steps before to produce the other ones.

3.2. Collisions between Gliders

Coding glider positions to get a desired reaction is a well-known solution for some related problems about complex behaviors. One of them is precisely the problem of self-organization (by structures Figure 13) [38]. In this way, we present how each basic glider can be produced by collisions between other different gliders.

A little bit more complicated is to obtain glider guns by collisions. Figure 14(a,b) depicts the production of a gun_2 from a multiple collision of gliders. Later on, we shall present two new combinations of guns [Figure 14(c,e)] and a new gun_4 [Figure 14(d)].

3.3. Other Collisions

A large variety of objects can be generated by collisions between gliders in $\phi_{R126maj:4}$. Some of these objects are useful for designing complex dynamical structures. For instance, Figure 15(a–c) shows how to delete (as an eater configuration) a single glider or a stream of gliders g_1 and g_2 . Two kinds of annihilations are depicted as well [see Figure 15(d,e)].

Figure 16 describes a number of black hole patterns emerging in $\phi_{R126maj:4}$. Traditionally a black hole is a Life object⁶ absorbing any glider that comes close to the main

⁶You can see a large classification of Life objects in <http://www.conwaylife.com/wiki/index.php>.

body (in this case, still life patterns). Its relevance consists of knowing how many patterns are able of attracting gliders and consuming all of them forever, in these cases the g_1 and g_2 gliders.

Figure 17 displays soliton reactions, where colliding gliders preserve their original forms. As known, a soliton has a small change in their phase and displacement; also soliton reactions are obtained with single gliders or by a stream of them.

The last set of examples (Figure 18) presents other binary reactions and some multiple collisions between g_1 and g_2 gliders. Some of them are conservative and others produce a new number of these structures. Finally, we can take some collisions to exploit their dynamics and controlling glider reactions (see an extended relations of collisions in Table 2). Thus, it can be obtained a full number of reactions for generating desired gliders. The set of collisions is useful as “raw material” in the implementation of computations on $\phi_{R126maj:4}$.

4. COMPUTING IN $\phi_{R126maj:4}$

Given the large number of reactions in $\phi_{R126maj:4}$ (see Table 2) the rule could be useful for implementing collision-based computing schemes [36, 39].

Figure 19 illustrates the interaction of gliders traveling, colliding one another, and implementing a Boolean conjunction as result. Initially from previous collisions we can embed logical constructions of AND and NOT gates from this figure, as follows:

- for the gate $(\neg a \wedge b)$ the implementation with $\phi_{R126maj:4}$ is in Figure 18(b); but only with one g_2 glider (see Table 2).
- for the gate $(a \wedge b)$ the implementation corresponds to Figure 13(a).

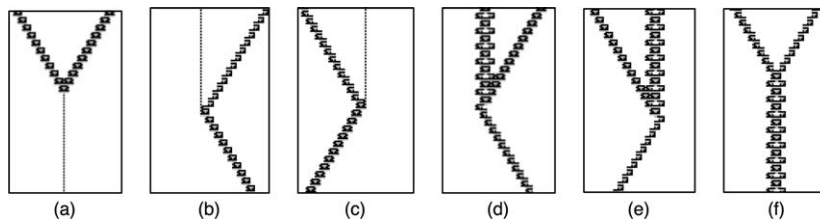
TABLE 1

Properties of Gliders $\mathcal{G}_{\phi_{R126maj:4}}$

Structure	v_g	Lineal volume	Mass
s_1	$0/2 = 0$	1	1
s_2	$0/10 = 0$	12	28
g_1	$3/5 \approx 0.6$	8	17
g_2	$-3/5 \approx -0.6$	8	17
gun_1	$0/19 = 0$	6	—
gun_2	$0/27 = 0$	6	—
gun_3	$0/110 = 0$	10	—
gun_4	$0/84 = 0$	15	—

Velocity v_g is calculated as displacement between period. The linear volume is the maximum distance between two cells in state ‘1’ (diameter of the set of cells in state ‘1’), finally mass is the number of cells in state ‘1.’

FIGURE 13



Generating basic gliders from collisions between other ones, this is self-organization by structures. The following reactions are illustrated as follows: (a) $g_1 + g_2 = s_1$, (b) $s_1 + g_2 = g_1$, (c) $g_1 + s_1 = g_2$, (d) $s_2 + g_2 = g_1$, (e) $g_2 + s_1 = g_2$, and (f) $g_1 + g_2 = s_2$.

- for the gate $(a \wedge \neg b)$ the implementation is presented in Figure 18(a); but only with one g_1 glider (see Table 2).
- for one FANOUT gate $(a \leftrightarrow b = a + a + b)$ the implementation is shown in Figure 18(d).

Indeed, here we also adopt ideas developed by Rennard in his design of Life computing architectures [40]. Glider g_1 represents value 0, two g_1 gliders together represent a value 1. Two gliders $2g_2$ traveling in positive direction describe the

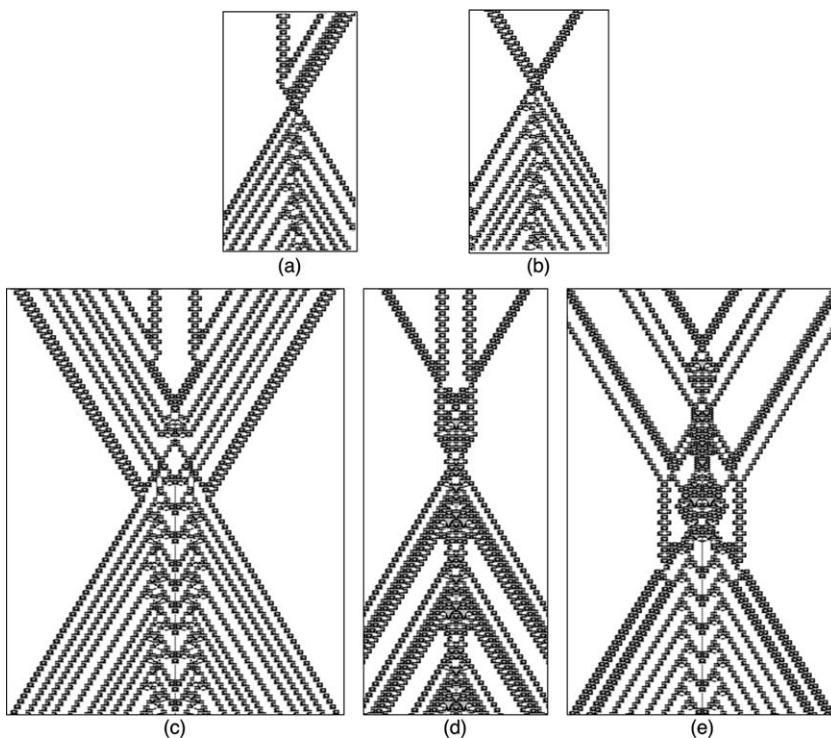
operator and one the register. Thus, the register will read FALSE OR TRUE if they are produced successfully.

Figure 20 illustrates the basic reactions required to produce a primitive computational scheme in $\phi_{R126maj;4}$. The following set of relations is applied (see Table 2):

$$2g_1 \leftrightarrow 2g_2 = \epsilon \quad g_1 \leftrightarrow 2g_2 = g_1 \quad g_1 \leftrightarrow 2g_2 = 2g_2 + g_1$$

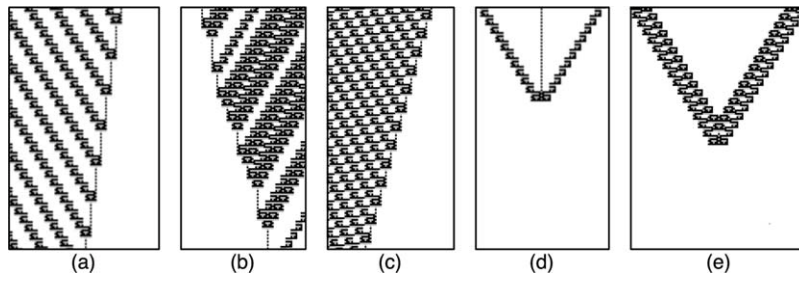
$$2g_1 \leftrightarrow 2g_2 = g_1 \quad 2g_1 \leftrightarrow 2g_2 = 2g_2 + 2g_1$$

FIGURE 14



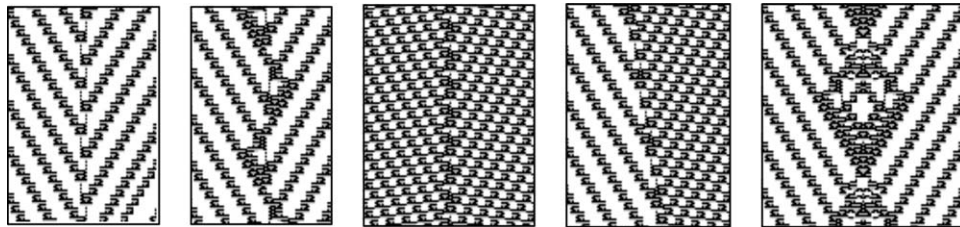
Generating gliders guns by collisions.

FIGURE 15



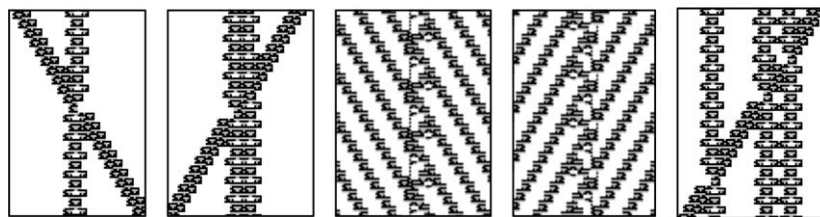
Eater reactions between gliders and still life (a, b, and c) and annihilation of gliders by collisions (d and e).

FIGURE 16



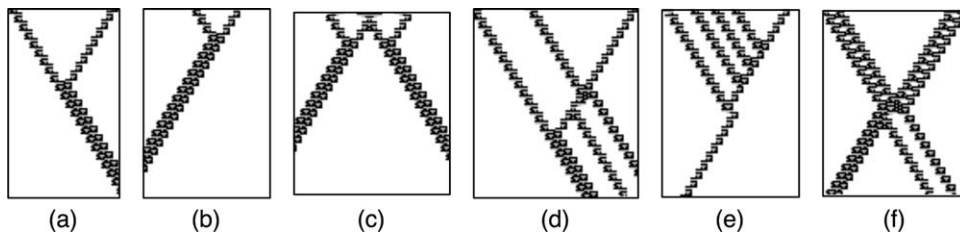
Black hole patterns consuming g_1 and g_2 gliders.

FIGURE 17



Examples of soliton reactions.

FIGURE 18



Examples of other collisions.

TABLE 2

Table of binary, multiple, and other collisions.

Summary of collisions in $\phi_{R126maj:4}$			
Binary	Multiple	Soliton	Guns
$s_1 \leftarrow g_2 = s_1$	$s_2 \leftarrow g_2 = 2g_1$	$g_1 \rightarrow s_1 = s_1 + g_1$	$s_1 \leftarrow 2g_2 = \text{gun}_1$
$g_1 \rightarrow s_1 = s_1$	$g_1 \rightarrow s_2 = 2g_2$	$s_1 \leftarrow g_2 = g_2 + s_1$	$\text{gun}_2 \leftarrow g_2 = \text{gun}_1$
$s_1 \leftarrow g_2 = g_1$	$s_2 \leftarrow 2g_2 = 2g_1$	$2g_1 \rightarrow s_2 = s_2 + 2g_1$	$g_1 \leftrightarrow g_2 \leftarrow 2g_2 = \text{gun}_2$
$g_1 \rightarrow s_1 = g_2$	$2g_1 \rightarrow s_2 = 2g_2$	$s_2 \leftarrow 2g_2 = 2g_2 + s_2$	$g_1 \leftrightarrow g_2 = \text{gun}_3$
$s_2 \leftarrow g_2 = g_1$	$s_2 \leftarrow 2g_2 = 2g_1 + g_2$	$2g_1 \rightarrow 2s_2 = 2g_1 + 2s_2$	$2g_1 \leftrightarrow 2g_2 = \text{gun}_2^*$
$g_1 \rightarrow s_2 = g_2$	$2g_1 \rightarrow s_2 = g_1 + 2g_2$	$2s_2 \leftarrow 2g_2 = 2g_2 + 2s_2$	$3g_1 \leftrightarrow 3g_2 = \text{gun}_1^*$
$g_1 \leftrightarrow g_2 = \emptyset$	$2g_1 \leftrightarrow 2g_2 = \emptyset$	$2g_1 \leftrightarrow 2g_2 = 2g_2 + 2g_1$	(* means gun composed)
$g_1 \leftrightarrow g_2 = s_1$	$2g_1 \leftrightarrow 2g_2 = g_1$		
$g_1 \leftrightarrow g_2 = s_2$	$2g_1 \leftrightarrow 2g_2 = g_2$		
$g_1 \leftrightarrow g_2 = g_1$	$2g_1 \leftrightarrow 2g_2 = 2g_1$		
$g_1 \leftrightarrow g_2 = g_2$	$2g_1 \leftrightarrow 2g_2 = 2g_2$		
$g_1 \leftrightarrow g_2 = 2g_1$	$g_1 \leftrightarrow 2g_2 = g_1$		
$g_1 \leftrightarrow g_2 = 2g_2$	$2g_1 \leftrightarrow g_2 = g_2$		
$g_1 \leftrightarrow g_2 = g_2 + 2g_1$	$g_1 \leftrightarrow 2g_2 = g_2$		
$g_1 \leftrightarrow g_2 = g_1 + 2g_2$	$2g_1 \leftrightarrow g_2 = g_1$		
	$g_1 \leftrightarrow 2g_2 = \emptyset$		
	$2g_1 \leftrightarrow g_2 = \emptyset$		
	$g_1 \leftrightarrow 2g_2 = 2g_2 + g_1$		
	$2g_1 \leftrightarrow g_2 = g_2 + 2g_1$		
	$g_1 \leftrightarrow 2g_2 = 2g_2 + 2g_1$		
	$g_1 \leftrightarrow 2g_2 = 2g_2 + g_2 + 2g_1$		
	$2g_1 \leftrightarrow g_2 = 2g_2 + 2g_1$		
	$2g_1 \leftrightarrow g_2 = 2g_2 + 2g_1 + g_1$		
	$3g_1 \leftrightarrow 3g_2 = 2g_1$		
	$g_1 \rightarrow s_1 \leftarrow g_2 = \emptyset$		
	$g_1 \rightarrow s_1 \leftarrow g_2 = s_1$		
	$g_1 \rightarrow 2s_2 \leftarrow g_2 = g_1 + g_2$		
	$g_1 \rightarrow 2s_2 \leftarrow g_2 = g_2 + g_1$		
	$2g_1 \rightarrow s_1 \leftarrow 2g_2 = 2g_2 + 2s_2 + 2g_1$		
	$3g_1 \leftrightarrow 3g_2 = g_2 + 2g_2 + 2g_1$		
	$4g_1 \leftrightarrow g_2 = 2g_1 + g_1$		
	$g_1 \leftrightarrow 4g_2 = g_2 + 2g_2$		

so we can represent serial reactions as:

$$\begin{aligned}
 2g_1 + 2g_2 &= \epsilon && \text{empty word} \\
 2g_1 + 2g_2 &= g_1 && \text{FALSE} \\
 2g_1 + 2g_2 &= 2g_1 && \text{TRUE.}
 \end{aligned}$$

and a NOT gate can be represented as:

- $\text{FALSE} + 2g_2 = \text{TRUE} + 2g_2$, or
- $\text{TRUE} + 2g_2 = \text{FALSE} + 2g_2$.

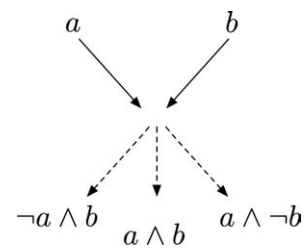
4.1. Constructing Formal Languages Since Gliders Collisions

in $\phi_{R126maj:4}$

To be considered as a mathematical machine, $\phi_{R126maj:4}$ should compute sets of formal languages [41]. We consider such implementation as an easy way to illustrate how implement some collision-based processes in $\phi_{R126maj:4}$ (Figure 21).

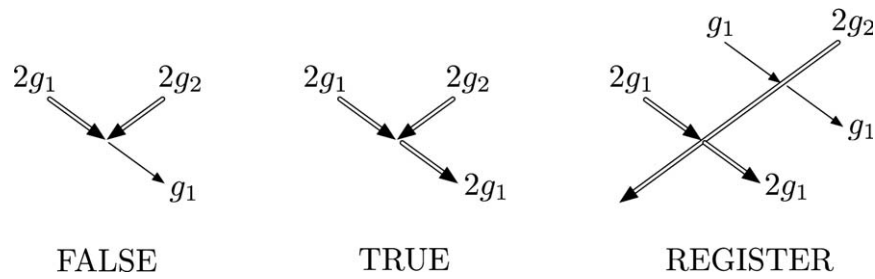
Let Σ be a nonempty finite alphabet. Thus, a string over Σ is a finite sequence of symbols from Σ . A set of all strings over Σ of length n is denoted by Σ^n . For example, if $\Sigma = \{0, 1\}$, then $\Sigma^2 = \{00, 01, 10, 11\}$ to

FIGURE 19



Colliding interactions deriving in logic gates.

FIGURE 20



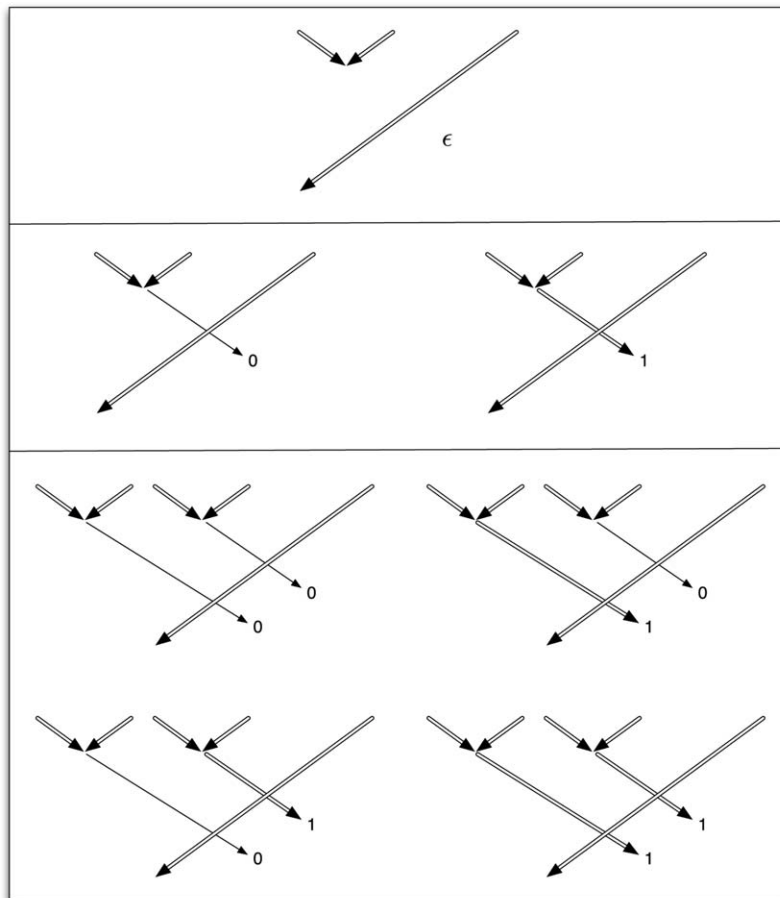
Example of devices working as data, operator, and register, respectively, by gliders in $\mathcal{G}_{\phi_{R126maj:4}}$.

$\Sigma^3 = \{000, 001, 010, 011, 100, 101, 110, 111\}$, and so on. This way $\Sigma^0 = \{\epsilon\}$ for any alphabet Σ . The set of all strings over Σ of any length is the Kleene closure of Σ and is denoted as Σ^* . However, we can write such expression in terms of Σ^n , as follows:

$$\Sigma^* = \bigcup_{n \in \mathbb{Z}_0} \Sigma^n. \quad (8)$$

This way for a binary alphabet $\Sigma^* = \{\epsilon, 0, 1, 00, 01, 10, 11, 000, 001, \dots\}$. Finally, a set of strings on Σ is called a formal language.

FIGURE 21



Constructing the formal collision-based languages in $\phi_{R126maj:4}$. They are Σ^0 (top), Σ^1 (middle), and Σ^2 (bottom).

Making use of gliders in $\phi_{R126maj:4}$ we can get any set of strings of Σ^* . For example, for the formal language 1^* we need to code all the initial conditions with reactions TRUE. For the formal language $(00 + 11)^*$ the initial condition will be coded as: $(g_1g_1 + 2g_12g_1)^*$. To yield an arbitrary length of strings, we increase the number of cells in the CA. All distances between gliders must be preserved and the left part become periodic.

5. CONCLUSIONS

We have enriched ECA Rule 126 with majority memory and have demonstrated that by applying certain filtering procedures we can extract rich dynamics of gliders, guns and infer a sophisticated system of reactions between gliders. We have discovered how a complex dynamics emerges from a chaotic system selecting an adequate memory. We have

shown that the majority memory increases nominal complexity but decreases statistical complexity of patterns generated by the CA. By applying methods such as de Bruijn diagrams, cycles, and graph theory, we have proved that Rule 126 with memory opens a new spectrum of complex rules, in this case a new CA with memory: $\phi_{R126maj:4}$. Finally, we have demonstrated some capacities for computing specific logical and memory functions, and a future work will be constructing a universal device.

ACKNOWLEDGMENTS

Genaro J. Martínez and Ramon Alonso-Sanz are supported by EPSRC (grants EP/F054343/1 and EP/E049281/1). Juan C. Seck-Tuoh-Mora is supported by CONACYT (project CB-2007/83554).

REFERENCES

1. Alonso-Sanz, R.; Martin, M.C.; Martin, M. The effect of memory in the spatial continuous-valued prisoner's dilemma. *Int J Bifurcation Chaos* 2001, 11, 2061–2083.
2. Alonso-Sanz, R.; Martin, M. One-dimensional cellular automata with memory: Patterns starting with a single site seed. *Int J Bifurcation Chaos* 2002, 12, 205–226.
3. Alonso-Sanz, R. Reversible cellular automata with memory. *Physica D* 2003, 175, 1–30.
4. Alonso-Sanz, R.; Martin, M. Elementary CA with memory. *Complex Syst* 2003, 14, 99–126.
5. Alonso-Sanz, R. Elementary rules with elementary memory rules: The case of linear rules. *J Cell Automata* 2006, 1, 71–87.
6. Alonso-Sanz, R. Memory boosts cooperation in the structurally dynamic prisoner's dilemma. *Int J Bifurcation Chaos* 2009, 19, 2899–2926.
7. Martínez, G.J.; Adamatzky, A.; Alonso-Sanz, A.; Seck-Tuoh-Mora, J.C. Complex dynamics emerging in Rule 30 with majority memory. *Complex Syst* 2010, 18, 345–365.
8. Martínez, G.J.; Adamatzky, A.; Alonso-Sanz, A. Complex dynamics of elementary cellular automata emerging from chaotic rules. *Int J Bifurcation Chaos*, in press.
9. Wolfram, S. *Cellular Automata and Complexity*; Addison-Wesley Publishing Company: Englewood Cliffs, NJ, USA, 1994.
10. Wuensche, A. Complexity in one-d cellular automata; Santa Fe Institute working paper 94-04-025, 1994.
11. Wolfram, S. Statistical mechanics of cellular automata. *Rev Mod Phys* 1983, 55, 601–644.
12. Wolfram, S. *A New Kind of Science*; Wolfram Media, Inc.: Champaign, Illinois, 2002.
13. McIntosh, H.V. *One Dimensional Cellular Automata*; Luniver Press: UK, 2009.
14. Martínez, G.J.; McIntosh, H.V.; Seck Tuoh Mora, J.C.; Chapa Vergara, S.V. Determining a regular language by glider-based structures called phases f_{i-1} in Rule 110. *J Cell Automata* 2008, 3, 231–270.
15. Martínez, G.J.; Adamatzky, A.; McIntosh, H.V. On the representation of gliders in Rule 54 by de Bruijn and cycle diagrams. *Lecture Notes Comput Sci* 2008, 5191, 83–91.
16. Minsky, M. *Computation: Finite and Infinite Machines*; Prentice Hall: Englewood Cliffs, NJ, USA, 1967.
17. Wolfram, S. Universality and complexity in cellular automata. *Physica D* 1984, 10, 1–35.
18. Ilachinski, A. *Cellular Automata. A Discrete Universe*; World Scientific Publishing: Mainland Press, Singapore, 2001.
19. Adamatzky, A. *Identification of Cellular Automata*; Taylor & Francis: UK, 1994.
20. Wolf-Gladrow, D.A. *Lattice-Gas Cellular Automata and Lattice Boltzmann Models*; Springer-Verlag Berlin: Heidelberg, Germany, 2000.
21. Kauffman, S.A. Emergent properties in random complex automata. *Physica D* 1984, 10, 145–156.
22. Rohlf, T.; Jost, C. A new class of cellular automata: How spatio-temporal delays affect dynamics and improve computation. *European Conference on Complex Systems* 2009, <http://cssociety.org/tiki-index.php?page=ECSS09-149>.
23. Letourneau, P.-J. <http://demonstrations.wolfram.com/OuterTotalistic2DCellularAutomataWithMemory/>, and <http://www.wolframscience.com/conference/2006/presentations/materials/letourneau.pdf>, 2007.
24. Xuelog, Z.; Qianmu, L.; Manwu, X.; Fengyu, L. A symmetric cryptography based on extended cellular automata. *IEEE Int Conf Syst Mand Cybern* 2005, 1, 10–12.
25. Ganguly, N.; Maji, P.; Das, A.; Sikdar, B.P.; Chaudhury, P. Generalized multiple attractor cellular automata (GMACA) model for associative memory. *Int J Bifurcation Chaos* 2002, 16, 781–795.
26. Maji, P.; Chaudhury, P. Non-uniform cellular automata based associative memory: Evolutionary design and basins of attraction. *Inform Sci* 2008, 178, 2315–2336.
27. Wuensche, A. The ghost in the machine: Basins of attraction of random Boolean networks. *Artificial Life III*; Langton, C., Ed. Santa Fe Institute Studies in the Sciences of Complexity; Addison-Wesley: Reading, MA, 1994; pp. 465–501.
28. Hopfield, J.J. Neural networks and physical systems with emergent collective computational abilities. *Proc Natl Acad Sci USA* 1982, 79, 2554–2558.
29. McIntosh, H.V. Wolfram's Class IV and a Good Life. *Physica D* 1990, 45, 105–121.
30. Wuensche, A.; Lesser, M. *The Global Dynamics of Cellular Automata*. Santa Fe Institute Studies in the Sciences of Complexity; Addison-Wesley Publishing Company: USA, 1992.

31. Voorhees, B.H. *Computational Analysis of One-Dimensional Cellular Automata*, Vol. 15; World Scientific Series on Nonlinear Science, Series A, Uto-Print, Singapore, 1996.
32. Voorhees, B.H. Remarks on applications of De Bruijn diagrams and their fragments. *J Cell Automata* 2008, 3, 187–204.
33. Seck-Tuoh-Mora, J.C.; Chapa-Vergara, S.V.; Martínez, G.J.; McIntosh, H.V. Procedures for calculating reversible one-dimensional cellular automata. *Physica D* 2005, 202, 134–141.
34. Wuensche, A. Classifying cellular automata automatically. *Complexity* 1999, 4, 47–66.
35. Martínez, G.J.; McIntosh, H.V.; Seck Tuoh Mora, J.C. Gliders in Rule 110. *Int J Unconventional Comput* 2006, 2, 1–49.
36. Martínez, G.J.; Adamatzky, A.; McIntosh, H.V. Phenomenology of glider collisions in cellular automaton Rule 54 and associated logical gates. *Chaos Solitons Fractals* 2006, 28, 100–111.
37. Alonso-Sanz, R. *Cellular Automata with Memory*; Old City Publishing: Philadelphia, USA, 2009.
38. Kauffman, S.A. *The Origins of Order: Self-Organization and Selection in Evolution*; Oxford University Press: New York, 1993.
39. Adamatzky, A. *Collision-Based Computing*; Springer-Verlag: London, UK, 2002.
40. Rennard, J.P. Implementation of logical functions in the game of life. *Collision-Based Computing*; Adamatzky, A., Ed. Springer-Verlag: London, UK, 2002; pp. 491–512.
41. Arbib, M.A. *Theories of Abstract Automata*; Prentice-Hall Series in Automatic Computation, Upper Saddle River, NJ, USA, 1969.